Surface impedance and reflectivity of superconductors

Physikalisch-Technische Bundesanstalt, D-3300 Braunschweig, West Germany

(Received 25 April 1989; accepted for publication 10 August 1989)

A complete solution to the Mattis-Bardeen equations of the anomalous skin effect in superconductors [Phys. Rev. 111, 412 (1958)] is presented in the case of plane, bulk conductors. This solution shows good agreement with existing solutions in the microwave region, and for the first time, it correctly describes measurements in the far-infrared region. It turns out that the solution to the Mattis-Bardeen equations for the extreme anomalous limit cannot be used for a correct description of experimental results. In addition, our exact solution is also applicable to strong-coupling superconductors.

I. INTRODUCTION

The theory of superconducting metals by Mattis and Bardeen¹ describes the electromagnetic behavior of superconductors in the weak-coupling limit. In a complete solution to this theory for plane, bulk superconductors, all the information can be summarized in the surface impedance Z.

Below the gap frequency, i.e., for photon energies ha lower than energy gap 2Δ , this may be shown by experiments on resonant cavities or strip lines. Here in the microwave region, good agreement exists between measurements on resonant cavities and calculations of solutions by Halbritter² and Turneaure.³ In the case of thin-film superconducting strip lines, much work has been done by Swihart4 and Kautz, 5,6 taking into account the classic and the extreme anomalous skin effect.

Above the gap frequency $(\hbar\omega > 2\Delta)$ no exact solution to the Mattis-Bardeen theory has yet been published. Just after publication of this theory, Miller⁷ presented an approximate solution containing the whole frequency region by using expansions in power series and neglecting the influence of the mean free path. But in most cases when measurement results of the absorption in bulk superconductors and the transmission through superconducting films were compared with theory, the much simpler solution of the extreme anomalous limit was applied. In the far-infrared region this had led to apparent discrepancies between theory and measurement, and these discrepancies have been thought to be due to the strong-coupling nature of the superconductors. However, it will be shown that they are indeed due to the improper approximation to the Mattis-Bardeen theory.

We begin the solution to the Mattis-Bardeen equations in Sec. II and the simplification of this solution to the extreme anomalous limit in Sec. III. A comparison between some important experimental and theoretical results and the derived equations is treated in Sec. IV A for the microwave region and in Sec. IV B for the far-infrared region.

Building on the present paper, we wish to present our experimental and more accurate theoretical results in the field of superconducting strip lines in another publication. This will be important for the correct calculation of integrated circuits such as voltage standards in our laboratory and may be of interest in the application of high- T_c superconductors.

II. SOLUTION FOR THE BULK LIMIT

As an expansion of the BCS description of superconductivity.8 the theory of Mattis and Bardeen includes the frequency dependence of magnetic fields. It provides a relationship between the total current density J and the vector potential A:

$$\mathbf{J}(\mathbf{r}) = \frac{3}{4\pi^2 v_0 \hbar \lambda_{L0}^2} \int_{V} \frac{\mathbf{RRA}(\mathbf{r}') I(\omega, R, T) e^{-R/I}}{R^4} dV', \quad (1)$$

with

$$\begin{split} I(\omega,\!R,\!T) &= -j\pi \int_{\Delta-\hbar\omega}^{\Delta} \big[1 - 2f(E + \hbar\omega)\big] \big[g(E)\cos\alpha\Delta_2 - j\sin\alpha\Delta_2\big] e^{j\alpha\Delta_1} \, dE \\ &- j\pi \int_{\Delta}^{\infty} \big[1 - 2f(E + \hbar\omega)\big] \big[g(E)\cos\alpha\Delta_2 - j\sin\alpha\Delta_2\big] e^{j\alpha\Delta_1} \, dE \\ &+ j\pi \int_{\Delta}^{\infty} \big[1 - 2f(E)\big] \big[g(E)\cos\alpha\Delta_1 + j\sin\alpha\Delta_1\big] e^{-j\alpha\Delta_2} \, dE, \end{split}$$

where $\Delta_1 = (E^2 - \Delta^2)^{1/2}$, $\Delta_2 = [(E + \hbar\omega)^2 - \Delta^2]^{1/2}$, $g(E) = (E^2 + \Delta^2 + \hbar\omega E)/(\Delta_1\Delta_2)$, and $\alpha = R/(\hbar v_0)$. $\mathbf{R} = \mathbf{r} - \mathbf{r}'$ is the vector from the point for which the current density is to be calculated to the volume element dV' assum-

ing homogeneity. $v_0 = l/\tau$ is the Fermi velocity with l the mean free path of the electrons and τ the relaxation time. The net effect of scattering is introduced by an extra factor of $\exp(-R/l)$ into the kernel of the integral for the current

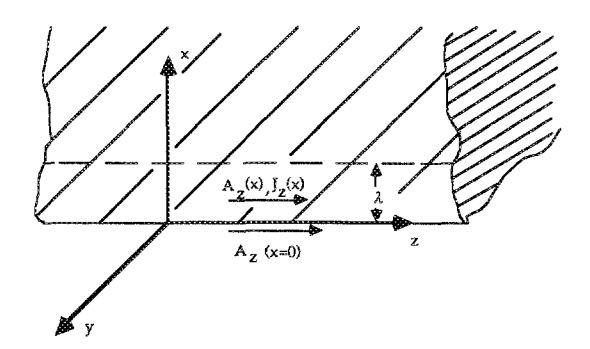


FIG. 1. Bulk and plane superconductor.

density in Eq. (1). \Re is the Planck constant divided by 2π , λ_{L0} the London penetration depth at a T=0 K described in Ref. 8, ω the circular frequency, and $f(E) = 1/[1 + \exp(E/E)]$ $(k_B T)$ the Fermi function with E the energy relative to the Fermi energy E_F and k_B the Boltzmann constant.

Considering a plane, bulk superconductor with an incident plane wave as shown in Fig. 1, and introducing a onedimensional Fourier transformation for the current density and the vector potential,

$$J_{z}(x) = \int_{-\infty}^{+\infty} J_{z}(q)e^{jqx} dq,$$

$$A_{z}(x) = \int_{-\infty}^{+\infty} A_{z}(q)e^{jqx} dq,$$
(2)

the Fourier component $A_{\tau}(q)$ can be removed from the integral in Eq. (1), leading to

$$J_z(q) = -K(q)A_z(q), (3)$$

which is a local relationship in Fourier space.

For the Mattis-Bardeen kernel K(q) one finds

$$K(q) = -\frac{3}{4\pi v_0 \hbar \lambda_{L0}^2} \int_0^{\infty} \int_{-1}^{+1} (1 - u^2) I(\omega, R, T) \times e^{jqRu} e^{-R/l} du dR,$$
(4)

an equation already mentioned by Tinkham.9

The integration with respect to u can easily be carried

$$\int_{-1}^{+1} (1 - u^2) e^{jqRu} du$$

$$= \frac{4}{(qR)^2} \left(\frac{\sin(qR)}{qR} - \cos(qR) \right)$$
(5)

and the substitution qR = x the kernel K(q) becomes

$$K(q) = -\frac{3}{\pi \hbar v_0 \lambda_{L0}^2 q} \int_0^\infty \left(\frac{\sin x}{x^3} - \frac{\cos x}{x^2} \right)$$
$$\times I(\omega, x/q, T) e^{-x/qt} dx. \tag{6}$$

Considering $I(\omega, x/q, T)$ in Eq. (1) we must make a distinction between $\hbar\omega < 2\Delta$ and $\hbar\omega > 2\Delta$. At photon energies below the energy gap, g(E) goes to infinity at $E = \Delta - \hbar \omega$ and at $E = \Delta$. In the integration inteval from $\Delta - \hbar \omega$ to Δ , the square root of Δ_1 becomes negative and has to be replaced by $\pm j|\Delta_1|$. At photon energies above the energy gap, g(E) additionally goes to infinity at $E = -\Delta$. The first integral of $I(\omega, x/q, T)$ in Eq. (1) must therefore be split into two parts, and the square root of Δ_1 is negative in the integration region from $-\Delta$ to Δ .

Noting this and splitting $I(\omega, x/q, T)$ into real and imaginary parts we get

 $\text{Re}[I(\omega,x/q,T)]$

$$= -\frac{\pi}{2} \int_{\Delta - \hbar\omega}^{-\Delta} [1 - 2f(E + \hbar\omega)] \{ [g(E) + 1] \sin(a^{-}x) - [g(E) - 1] \sin(a^{+}x) \} dE$$

$$-\pi \int_{\Delta - \hbar\omega, -\Delta}^{\Delta} [1 - 2f(E + \hbar\omega)] \left(\frac{E^{2} + \Delta^{2} + \hbar\omega E}{(\Delta^{2} - E^{2})^{1/2} [(E + \hbar\omega)^{2} - \Delta^{2}]^{1/2}} \cos(a_{2}x) + \sin(a_{2}x) \right) e^{-a_{1}x} dE$$

$$+\pi \int_{\Delta}^{\infty} [1 - f(E) - f(E + \hbar\omega)] [g(E) - 1] \sin(a^{+}x) dE - \pi \int_{\Delta}^{\infty} [f(E) - f(E + \hbar\omega)] [g(E) + 1] \sin(a^{-}x) dE$$
(7)

5951

$$Im[I(\omega,x/q,T)] = +\frac{\pi}{2} \int_{\Delta-\hbar\omega}^{-\Delta} [1 - 2f(E + \hbar\omega)] \{ [g(E) + 1]\cos(a^{-}x) + [g(E) - 1]\cos(a^{+}x) \} dE$$
$$-\pi \int_{\Delta}^{\infty} [f(E) - f(E + \hbar\omega)] \{ [g(E) + 1]\cos(a^{-}x) + [g(E) - 1]\cos(a^{+}x) \} dE, \tag{8}$$

with $a^+ = a_1 + a_2$, $a^- = a_2 - a_1$, $a_1 = \Delta_1/(\hbar w_0 q)$, and $a_2 = \Delta_2/(\hbar v_0 q)$.

Below the gap frequency ($\hbar\omega < 2\Delta$), the first integrals in Eqs. (7) and (8) must be set to zero, and the lower integration limit of the second integral in Eq. (7) is $\Delta - \hbar \omega$. Above the gap frequency all integrals must be taken into account, and the lower limit of the second integral in Eq. (7) becomes $-\Delta$.

After $I(\omega, x/q, T)$ has been inserted into the Mattis-Bardeen kernel K(q), the following integrals can be derived:

$$\int_0^\infty e^{-bx} \left(\frac{\sin x}{x^3} - \frac{\cos x}{x^2} \right) \cos(ax) dx = R(a,b)$$
 (9)

$$\int_0^\infty e^{-bx} \left(\frac{\sin x}{x^3} - \frac{\cos x}{x^2} \right) \sin(ax) dx = S(a,b)$$
 (10)

with b = 1/ql. With the help of partial integration they can be transformed into tabulated integrals (Ref. 10 and Gröbner and Hofreiter¹¹). The solutions are

$$R(a,b) = -\frac{b}{2} + \frac{ab}{4} \ln \left(\frac{b^2 + (1+a)^2}{b^2 + (1-a)^2} \right) + \frac{1}{4} (1+b^2 - a^2) \left[\arctan \left(\frac{2b}{b^2 + a^2 - 1} \right) + n_x \pi \right],$$

$$(11)$$

$$S(a,b) = \frac{a}{2} - \frac{ab}{2} \left[\arctan \left(\frac{2b}{b^2 + a^2 - 1} \right) + n_x \pi \right]$$

$$+ \frac{1}{8} (1 + b^2 - a^2) \ln \left(\frac{b^2 + (1+a)^2}{b^2 + (1-a)^2} \right),$$

$$n_x = \begin{cases} 0 & \text{for } b^2 + a^2 - 1 \ge 0 \\ 1 & \text{for } b^2 + a^2 - 1 < 0 \end{cases}$$

$$(12)$$

With b=0 (infinitely large mean free path l), Eqs. (11) and (12) are reduced to the corresponding equations published by Miller [Ref. 7, Eq. (13)]. Furthermore, he derived approximate formulas for the kernel K(q) for large and small q, expanding K(q) in power series.

The solution of the exact kernel K(q) finally becomes

$$= \frac{3}{\hbar w_0 \lambda_{L_0}^2 q} \left[\int_{\Delta - \hbar \omega, -\Delta}^{\Delta} \left[1 - 2f(E + \hbar \omega) \right] \left(\frac{E^2 + \Delta^2 + \hbar \omega E}{(\Delta^2 - E^2)^{1/2} [(E + \hbar \omega)^2 - \Delta^2]^{1/2}} R(a_2, a_1 + b) + S(a_2, a_1 + b) \right) dE$$

$$+ \frac{1}{2} \int_{\Delta - \hbar \omega}^{\Delta} \left[1 - 2f(E + \hbar \omega) \right] \left\{ [g(E) + 1] S(a^-, b) - [g(E) - 1] S(a^+, b) \right\} dE$$

$$- \int_{\Delta}^{\infty} \left[1 - f(E) - f(E + \hbar \omega) \right] [g(E) - 1] S(a^+, b) dE + \int_{\Delta}^{\infty} \left[f(E) - f(E + \hbar \omega) \right] [g(E) + 1] S(a^-, b) dE \right]$$
(13)

and

$$\operatorname{Im}\left[K(q)\right] = \frac{3}{\hbar v_0 \lambda_{L_0}^2 q} \left(-\frac{1}{2} \int_{\Delta - \hbar \omega}^{-\Delta} \left[1 - 2f(E + \hbar \omega)\right] \left\{ [g(E) + 1]R(a^-, b) + [g(E) - 1]R(a^+, b) \right\} dE + \int_{\Delta}^{\infty} \left[f(E) - f(E + \hbar \omega)\right] \left\{ [g(E) + 1]R(a^-, b) + [g(E) - 1]R(a^+, b) \right\} dE \right), \tag{14}$$

which is identical with the result of Turneaure³ for the special case of $\hbar\omega < 2\Delta$.

It can be shown that for the normal conducting state at $T = T_c$ and $2\Delta = 0$, Eqs. (13) and (14) lead to the particular result given by Mattis and Bardeen¹:

$$I(\omega, x/q, T_c) = -j\pi\hbar\omega e^{-j(x\omega/qv_0)}, \qquad (15)$$

which corresponds to a kernel $K_n(q)$ in the normal conducting state:

$$K_n(q) = \frac{3}{v_0 \lambda_{r,0}^2 q} \left[S(a_n, b) + jR(a_n, b) \right]$$
 (16)

with

$$a_n = \omega/v_0 q$$
, $b = 1/q l$.

Having solved the Mattis-Bardeen kernel K(q) we are now able to calculate the surface impedance using an equation of Reuter and Sondheimer¹² for diffuse scattering of the electrons at the surface of the conductor.

$$Z = j\omega\mu_0\pi \frac{1}{\int_0^\infty \ln[1 + K(q)/q^2]dq} = R + jX$$
$$= R + j\omega\mu_0\lambda. \tag{17}$$

Calculations for specular scattering have not been carried out in this paper, for both diffuse and specular scattering results are quite similar to each other and the produced surfaces seem to be more diffuse than specular. The surface

impedance Z contains all the information about the surface material available from the Mattis-Bardeen theory. The surface resistance R is a measure of conductor losses, and the surface reactance X is directly connected to the superconducting penetration depth λ .

III. EXTREME ANOMALOUS SKIN EFFECT

In the case of the extreme anomalous skin effect, the mean free path should be much greater than the skin penetration depth $(l \gg \delta)$, and the Pippard coherence length defined by $1/\xi = 1/\xi_0 + 1/\alpha l$ (α is the empirical constant) should be much greater than the superconducting penetration depth $(\xi \gg \lambda)$. Mattis and Bardeen described this case by setting $\alpha = R = 0$ in Eq. (1); therefore the kernel $I(\omega,0,T)$ follows as

$$\begin{aligned} \operatorname{Re}[I(\omega,0,T)] \\ &= -\pi \int_{\Delta-\hbar\omega,\ \Delta}^{\Delta} \left[1 - 2f(E + \hbar\omega)\right] \\ &\times \frac{E^2 + \Delta^2 + \hbar\omega E}{(\Delta^2 - E^2)^{1/2} [(E + \hbar\omega)^2 - \Delta^2]^{1/2}} dE, \\ \operatorname{Im}[I(\omega,0,T)] \end{aligned}$$

$$= \pi \int_{\Delta - \hbar \omega}^{\infty} [1 - 2f(E + \hbar \omega)] g(E) dE$$
$$-2\pi \int_{\Delta}^{\infty} [f(E) - f(E + \hbar \omega)] g(E) dE \qquad (18)$$

in the superconducting state, and as

$$I(\omega, 0, T_c) = -j\pi\hbar\omega \tag{19}$$

in the normal conducting state.

When $J_{\omega}/J_{n\infty}$ is calculated in the extreme anomalous limit using the Mattis-Bardeen integral in Eq. (1), the corresponding kernels $I(\omega,0,T)$ and $I(\omega,0,T_c)$ can be taken out of the integrals, and according to Glover and Tinkham¹³ a complex conductivity is introduced:

$$\frac{J_{\infty}}{J_{n\infty}} = \frac{I(\omega, 0, T)}{I(\omega, 0, T_c)} = \frac{\sigma_1^{-j} \sigma_2}{\sigma_n}, \tag{20}$$

where σ_n is the conductivity in the normal conducting state at a given frequency. The kernels $K_{\infty}(q)$ and $K_{n_{\infty}}(q)$ can then be written as

$$K_{\infty}(q) = -\frac{3}{4} \frac{I(\omega, 0, T)}{\hbar v_0 \lambda_{L0}^2 q} = \frac{3}{4} \frac{\pi \omega}{v_0 \lambda_{L0}^2 q} \left(\frac{\sigma_2}{\sigma_n} + j \frac{\sigma_1}{\sigma_n}\right)$$
(21)

and

5953

$$K_{n_{\infty}}(q) = j \frac{3}{4} \frac{\pi \omega}{v_0 \lambda_{L0}^2 q}$$
 (22)

IV. APPLICATIONS TO BULK SUPERCONDUCTORS

To calculate the surface impedance Z according to Eqs. (17), (13), and (14), a numerical double integration has to be carried out, and five material parameters are needed: the energy gap $2\Delta_0$ at T=0 K, the London penetration depth $\lambda_{L\,0}$ at T=0 K, the mean free path l, the critical temperature T_c , and the BCS coherence length ξ_0 or the Fermi velocity v_0 , related to each other by

$$\xi_0 = \hbar v_0 / \pi \Delta_0. \tag{23}$$

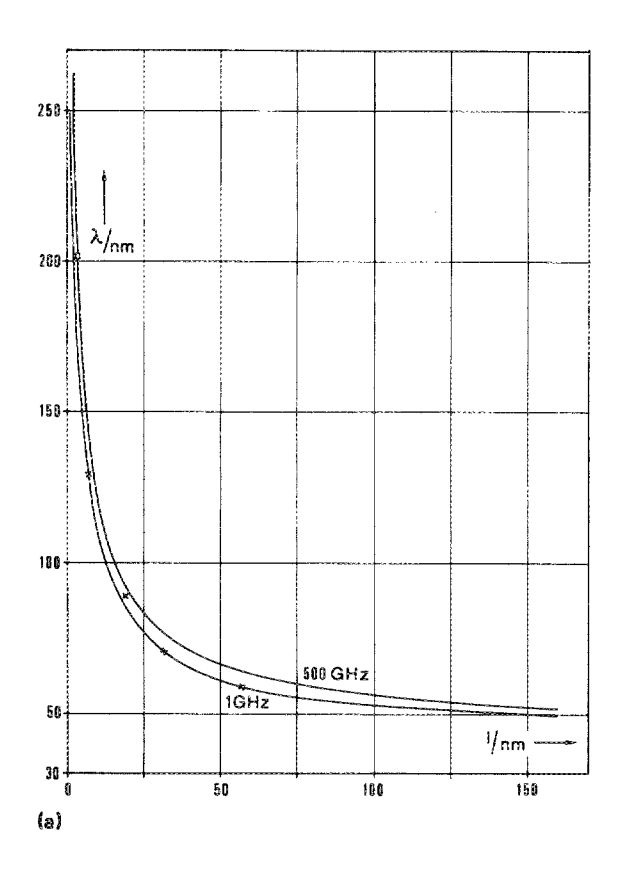
The temperature dependence of the energy gap is also needed. Suitable values are obtained from Mühlschlegel's calculations¹⁴ of the BCS temperature dependence or from the simple equation

$$\frac{2\Delta}{2\Delta_0} = \left[\cos\left(\frac{\pi}{2}t^2\right)\right]^{1/2},\tag{24}$$

with $t=T/T_c$, which deviates by only 2% from Mühlschlegel's tabulated values.

If all these parameters are introduced into a FORTRAN computer program, the surface impedances can be calculated for any circular frequency ω , for any mean free path l as long as only nonmagnetic impurities are involved, and for any temperature T.

Important conditions for the validity of the present solution are that the superconductors must be isotropic, bulk, and plane and the theory of Mattis and Bardeen is only valid for weak-coupling superconductors. Despite the last restriction a comparison of experimental and theoretical results shows that our solution to the Mattis-Bardeen equations is a



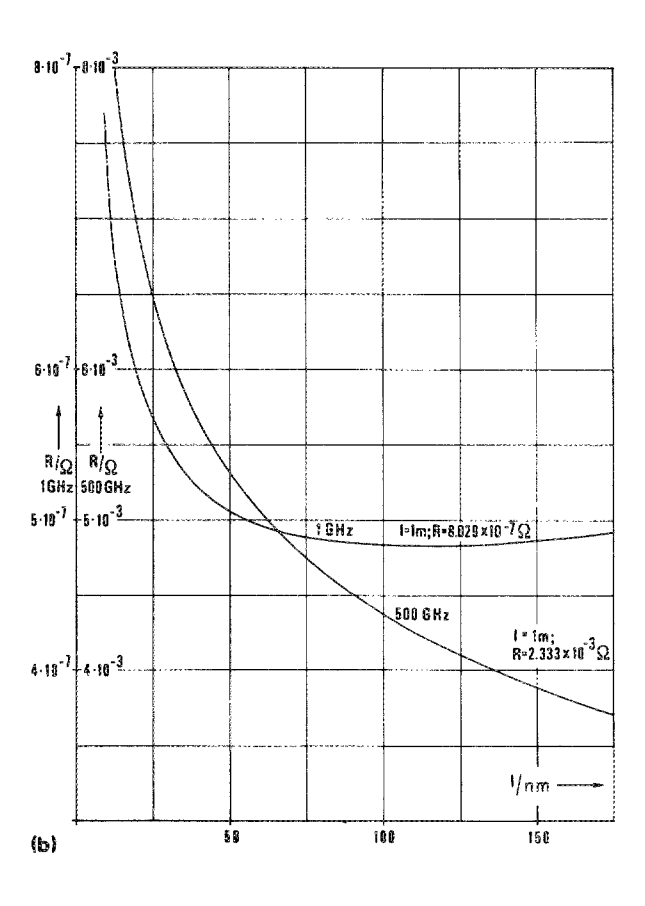


FIG. 2. (a) Superconducting penetration depth λ vs mean free path l for Pb at T=4.2 K; curves calculated with material parameters from Turneaure (Ref. 3) listed in Table I; \times , Hasse and Lachmann (Ref. 15); \bigcirc , Henkels and Kircher (Ref. 16). (b) Surface resistance vs mean free path for Pb at T=4.2 K.

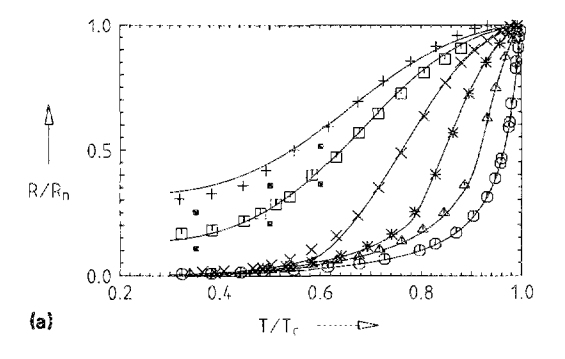
TABLE I. Material parameters.

	$2\Delta_0/k_BT_c$	$T_{c}(K)$	λ_{L0} (nm)	$v_0 (10^6 \text{m/s})$	ξ_0 (nm)	l(nm)	References
Pb	4.10	7.19	30.8	0.60	99	710	3
Pb	4.10	7.22	28.0	0.68	111	1000	25
Nb	3.80	9.20	33.3	0.28	39	20	22
Ai	3.25	1.178	15.4	1.34	1729	10 000	19
Al	3.37	1.178	16.0	1.23	1500	∞	7,8

good approach, even for the strong-coupling case (see the following sections).

A. Microwave region

As mentioned in Sec. II, in the region below the gap frequency ($\hbar\omega < 2\Delta$) the present solution is identical with that of Turneaure.³ Halbritter² also obtained an equivalent solution using a Green's function. Both theoretical results were able to describe measurements on resonant cavities in the microwave region correctly. For this reason we do not present here many experimental and theoretical results in the microwave region. As one example, Fig. 2 shows the dependence of the surface impedance Z on mean free path l.



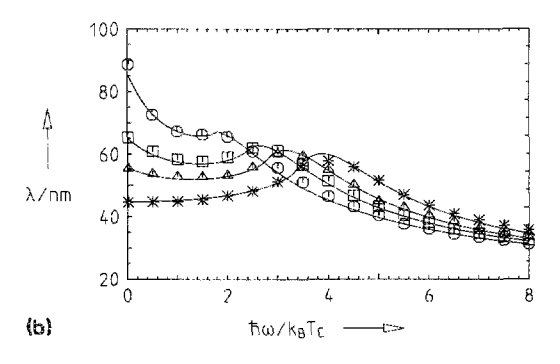


FIG. 3. (a) R/R_n vs T/T_c measured by Biondi and Garfunkel (Ref. 18); \bigcirc , $0.64k_BT_c$; \triangle , $1.66k_BT_c$; *, $2.46k_BT_c$; \times , $3.08k_BT_c$; \square , $3.63k_BT_c$; +, $3.91k_BT_c$; curves calculated using parameters from Ref. 16 except $2\Delta_0=3.40k_BT_c$; **3.** calculated by Miller (Ref. 7). (b) Superconducting penetration depth vs frequency calculated by Biondi and Garfunkel (Ref. 19); *, t=0; \triangle , t=0.7; \square , t=0.8; \bigcirc , t=0.9; curves calculated using parameters from Ref. 19 except $2\Delta_0=3.40k_BT_c$.

With increasing impurity content (decreasing mean free path *l*) the electromagnetic field penetrates more deeply into the conductor. This behavior is demonstrated by the solid line in Fig. 2(a), for lead at 4.2 K and 1 GHz, calculated with material parameters from Turneaure³ listed in Table I. The course of the superconducting penetration depth at 500 GHz (a frequency well below the gap frequency) is not much different from that at 1 GHz. Values measured by Hasse and Lachmann, ¹⁵ who used a lead cavity with up to 5 at % Bi at 9.58 GHz, are also included, as is a result of Henkels and Kircher¹⁶ obtained with Pb-Bi thin-film strip lines below 30 MHz.

At sufficiently low frequencies the surface resistance versus the mean free path shows a minimum at $l \approx \xi_0$, as has been noted and explained by Halbritter. ¹⁷ In Fig. 2(b) this minimum appears at 1 GHz but not at 500 GHz, where R increases to $8.9 \times 10^{-7} \Omega$ for l going to infinity.

A second example containing the frequency region below and above the gap frequency is shown in Fig. 3. Biondi and Garfunkel¹⁸ measured the ratio R/R_n (R is the surface resistance in the superconducting state and R_n the surface resistance in the normal conducting state at $T=T_c$) of aluminum over a wide range of frequency and temperature [data symbols in Fig. 3(a)]. From the values obtained they calculated the frequency dependence of the superconducting penetration depth at different temperatures using Kronig–Kramers integral transforms¹⁹ [data symbols in Fig. 3(b)].

The solid lines in Figs. 3(a) and 3(b) were obtained by using the material parameters given by Biondi and Garfunkel listed in Table I except the energy gap. This parameter was changed from $(3.25 \pm 0.1)k_BT_c$ to $3.40k_BT_c$ and $3.91k_BT_c$.

Trying to fit the experimental results of Biondi and Garfunkel, Miller⁷ used a similarly large energy gap $2\Delta_0$ of $3.37k_BT_c$ and parameters quite similar to those of Biondi and Garfunkel as listed in Table I, thus obtaining a similar good fit to the experiment, except to the regions at low temperatures and frequencies at the gap frequency [data points in Fig. 3(a)].

This can be seen in Fig. 4, where r/r_{∞} is drawn versus the photon energy $\hbar\omega$ in units of k_BT_c . r corresponds to R/R_n and $r_{\infty}=R_{\infty}/R_{n\infty}$ is the appropriate quotient in the extreme anomalous limit. Larger discrepancies between Miller's approximate solution (dashed lines) and the present solution (solid lines) appear at lower temperatures and frequencies around the gap frequency.

Unfortunately, there still remain some smaller deviations at low temperatures and frequencies at the gap frequen-

5954

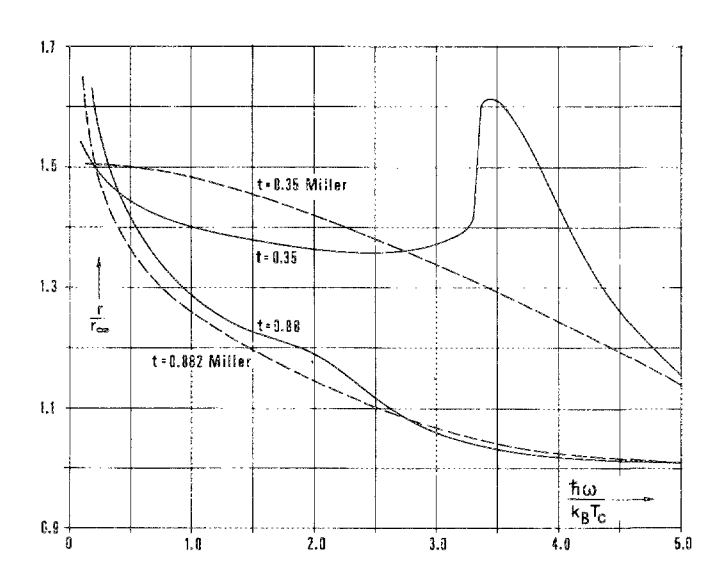


FIG. 4. Frequency dependence of r/r_{∞} , $r=R/R_n$, $r_{\infty}=R_{\infty}/R_{n,\infty}$ for Al; material parameters taken from Miller (Ref. 7); —, exact calculation; —, Miller's calculation.

cy, perhaps caused by anisotropy effects of the energy gap or measuring errors. This temperature and frequency range is also important for describing the measurement results of the absorption in bulk superconductors in the next section, where the present solution is well able to fit the experimental data on lead, lead alloys, and niobium specimens.

B. Far-infrared region

Many attempts have been made to fit the Mattis-Bardeen theory in the extreme anomalous limit (Sec. III) to experimental results in the far-infrared region for bulk material and thin films, but considerable discrepancies arose. The question to what extent this limit can be used for aluminum is also answered in Fig. 4. If the curves of r/r_{∞} ($r = R/R_n$, $r_{\infty} = R_{\infty}/R_{n\infty}$) reach a value of 1, the extreme anomalous

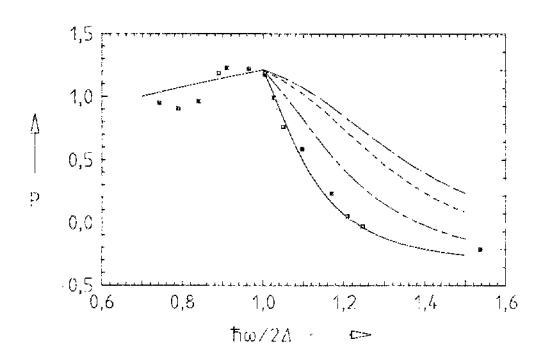


FIG. 6. Absorption spectrum of Pb–Tl 1 at. %; *, measured points from Leslie and Ginsberg (Ref. 20); —, extreme anomalous limit; —, local limit; —, calculated by Ginsberg (Ref. 21) using Leplaes theory (Ref. 22); —, exact calculation with material parameters from Turneaure (Ref. 3); $2\Delta_0 = 4.332k_BT_c$, l = 170 nm, K = 4.673, T = 1.3 K.

limit can be applied without error. Even for aluminum, which fulfills the conditions for the extreme anomalous limit quite well (see Sec. III and Biondi and Garfunkel¹⁹), according to Fig. 4 a satisfactory application is possible only at high frequencies and temperatures slightly lower than T_c .

In the case of lead, in Fig. 5 the deviations from the extreme anomalous limit become even larger. As shown, application of the extreme anomalous limit is off scale for photon energies below $6.0k_BT_c$ (corresponding to frequencies below 900 GHz). Similar curves for Sn calculated by Miller (Fig. 4 of Ref. 7) decrease continuously with increasing frequency and show no peaks at the gap frequencies. The disappearance of these peaks is a result of the interpolation in calculating the shape of the kernel K(q) between small and large q.9

Leslie and Ginsberg²⁰ measured the far-infrared absorption in bulk lead alloys. The data points in Fig. 6 show the result for Pb–Tl 1 at. %. The worst fit is obtained in the extreme anomalous limit (long-dashed line), and the local limit (short-dashed line) does not give a much better result.

Ginsberg²¹ later tried to fit his experiment with the help

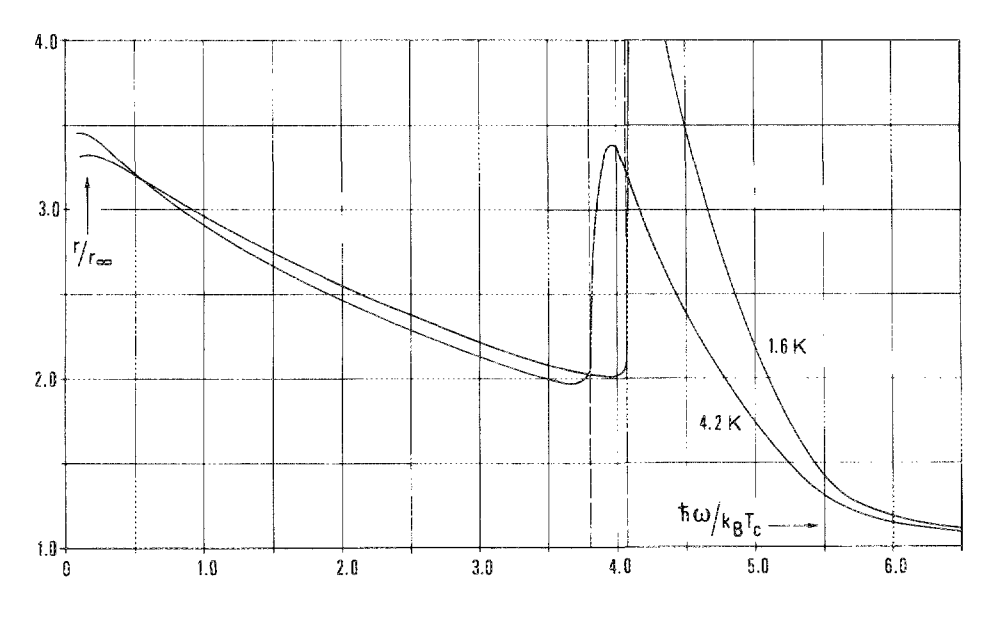


FIG. 5. Frequency dependence of r/r_{∞} for Pb; material parameters taken from Turneaure (Ref. 3); ---, corresponding gap frequencies.

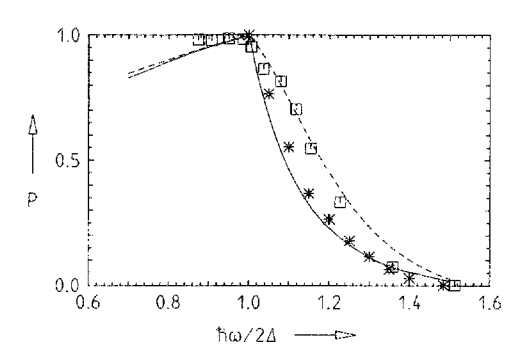


FIG. 7. Absorption spectra for two diluted Pb specimens: Pb-Bi 0.01 at. %; \Box , Pb-Bi 6 at. %, measured by Leslie and Ginsberg; —, $2\Delta_0=4.362k_BT_c$, l=9400 nm, K=6.803; —, $2\Delta_0=4.40k_BT_c$, l=16 nm, K=2.915; other parameters taken from Turneaure T=1.3 K.

of Leplae's theory²² (long- and short-dashed line in Fig. 6). The principle of this evaluation is to calculate Im[K(q)] in Eq. (14) at T=0 K by neglecting the second integral, to obtain Re[K(q)] by a Kramers-Kronig transform, and to calculate the surface impedance using Eq. (17). The only important difference to our calculations seem to be that the second integral in Eq. (14) is not considered, while taking T=0 K is quite well justified.

The solid line in Fig. 6 was obtained using Ginsberg's formula for the absorption formula

$$P = \frac{R_n - R}{R_n(\omega_g) + R/K},\tag{25}$$

where $R_n(\omega_g)$ is the surface resistance in the normal conducting state at the gap frequency and K is chosen so that the height of the absorption curve at ω_g is unity. It should be mentioned that we used no fitting parameter and the same value of K for this. Apart from the energy gap, Turneaure's material parameters for lead, which work well in the microwave region, and the mean free path measured by Leslie and Ginsberg²⁰ were used.

The measured absorption at frequencies below the gap frequency in Fig. 6 is not reproduced by the theory. Precursor peaks as in Fig. 6 have been observed in the absorption

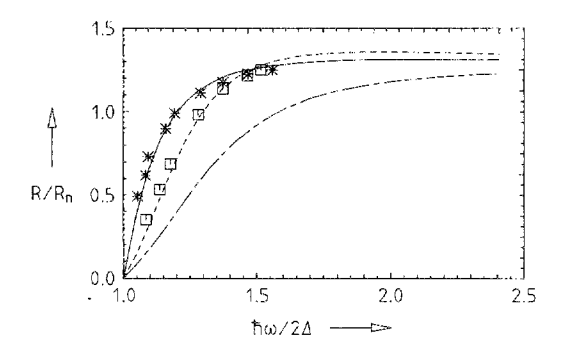


FIG. 8. Absorption spectra measured by Norman (Ref. 25): *, Pb; \square , Nb; -, $2\Delta_0 = 4.31k_BT_c$, parameters taken from Turneaure (Ref. 3); --, $2\Delta_0 = 3.60k_BT_c$, l = 9 nm; parameters taken from Bauer, Giordano, and Hahn (Ref. 27); ---, extreme anomalous limit.

and transmission spectra of Pb and Hg (Richards and Tinkham²³ and Ginsberg and Tinkham²⁴), and in one case described by assuming a second energy gap (Norman²⁵). In a later paper Norman and Douglass²⁶ showed that their measured precursor peaks were spurious and due to the unexpected presence of higher-order radiation in the beam of their monochromator. They suggested that a small amount of higher-order radiation was present also in other experiments; therefore all reported precursor peaks may be caused by artifacts.

Figure 7 also shows two experimental results obtained by Leslie and Ginsberg on a weakly and a strongly diluted specimen, again taking the measured values of $2\Delta_0$ and l, without using a fitting parameter.

The values measured by Norman²⁵ of lead and niobium above the gap frequency in Fig. 8 are also well described by the Mattis-Bardeen theory. For lead we again took all the material parameters of Turneaure except the measured energy gap. For niobium we took all the parameters from Bauer, Giordano, and Hahn²⁷ listed in Table I except the measured energy gap and the mean free path l, which was changed from l=20 nm to l=9 nm to get a better fit. This value corresponds with that estimated by Norman.

Bauer, Giordano, and Hahn used the parameters in Table I to describe their measurement results at a cavity between 1.7 and 7.8 GHz, and it should be mentioned that they observed a small but definite discrepancy of the frequency dependence between experiment and exact theory; this can be explained by using a continuously increasing energy gap (Philipp and Halbritter²⁸).

The solution to the Mattis-Bardeen equations in the extreme anomalous limit can only be used at very high frequencies. The approximate solution of Miller⁷ fails at low temperatures and frequencies surrounding the gap frequency, just in that region where absorption and transmission measurements are performed.

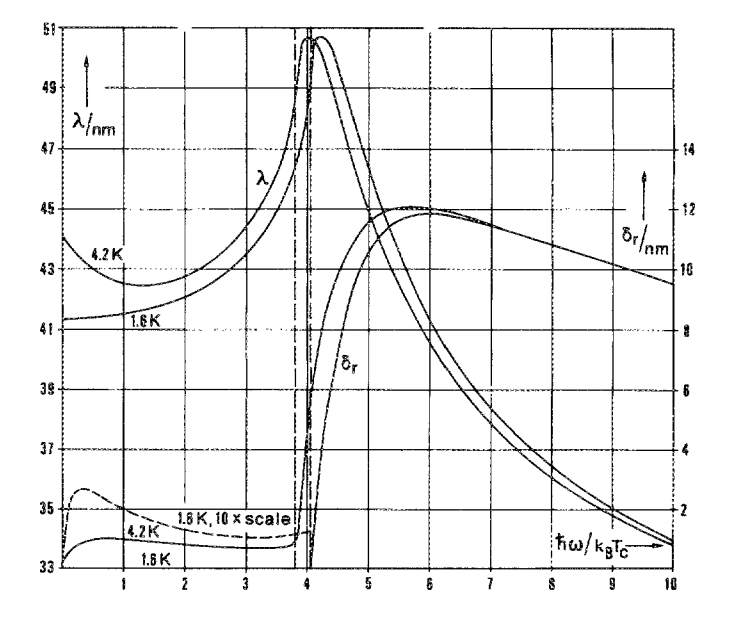


FIG. 9. Frequency dependence of the skin penetration depths λ and δ_r , parameters taken from Wilson (Ref. 30).

5956

As shown above, the solution to the Mattis-Bardeen equations is well qualified to describe measurement results of absorption spectra in the far-infrared region and also those of strong-coupling superconductors such as lead and lead alloys. Good agreement between measurements and calculations of lead in the microwave region have been reported by Turneaure³ and Bruynseraede et al.²⁹ Concluding this section, we are justified in showing the frequency dependence of the formally defined skin penetration depths

$$\lambda = X/\omega\mu_0,\tag{26}$$

$$\delta_r = R / \omega \mu_0 \tag{27}$$

for lead at 1.6 and 4.2 K in Fig. 9. The material parameters used to calculate these curves were taken from Wilson³⁰ (Table I) and are quite similar to those of Turneaure.

The curves for λ vs $\hbar\omega/(k_B T_c)$ show maxima at frequencies somewhat higher than the gap frequencies and reach the London penetration depths λ_L at very high frequencies. Below the gap frequency, the δ_r values remain small, increase strongly above the gap frequency, and finally reach the temperature-independent limit predicted by the theory of the anomalous skin effect in normal conductors by Chambers.³¹ That is, the Mattis-Bardeen theory includes the Chambers theory, as it has to.

V. CONCLUSION

The equations for the surface impedance of superconductors derived by Mattis and Bardeen are precisely solved for bulk conductors. This complete calculation shows very good agreement with measurements, not only in the microwave region but also in the far-infrared region, above the gap frequency, where the extreme anomalous limit cannot be used.

As shown before in the microwave region the absorption of bulk material consisting of strong-coupling superconductors can be described by using $\Delta/k_B T_c \geqslant 2$, although strictly speaking, the Mattis-Bardeen theory is only valid in the weak-coupling limit.

It has thus been shown that the exact solution to the Mattis-Bardeen theory describes the electromagnetic properties of superconductors for all frequencies, temperatures, and mean free paths (as long as only nonmagnetic impurities are involved), even for strong-coupling superconductors. Five material parameters are needed: the energy gap, the critical temperature, the London penetration depth, the Fermi velocity (or the BCS coherence length), and the mean free path.

ACKNOWLEDGMENTS

The author is indebted to Professor J. H. Hinken and to Professor V. Kose for their helpful comments and suggestions.

- ¹D. C. Mattis and J. Bardeen, Phys. Rev. 111, 412 (1958).
- ²J. Halbritter, Ph. D. thesis, Externer Bericht 3/69-2, Kernforschungs-Zentrum Karlsruhe (1969).
- ³J. P. Turneaure, Ph. D. thesis, Stanford University, Stanford, California (1967).
- ⁴J. C. Swihart, J. Appl. Phys. 32, 461 (1961).
- ⁵R. L. Kautz, J. Appl. Phys. 49, 308 (1978).
- ⁶R. L. Kautz, IEEE Trans. Magn. MAG-15, 566 (1979).
- ⁷P. B. Miller, Phys. Rev. 118, 928 (1960).
- ⁸J. Bardeen, L. N. Cooper, and J. R. Schrieffer, Phys. Rev. 108, 1175 (1957).
- ⁹M. Tinkham, in Low-Temperature Physics (McGraw-Hill, New York, 1966).
- ¹⁰R. Pöpel, Ph. D., University of Braunschweig, Braunschweig, West Germany (1986).
- ¹¹W. Gröbner and N. H. Hofreiter, Integraltafeln (Springer, Wien, 1966), Part II.
- ¹²G. E. H. Reuter and E. H. Sondheimer, Proc. R. Soc. (London) Ser. A 195, 336 (1948).
- ¹³R. E. Glover and M. Tinkham, Phys. Rev. 108, 243 (1957).
- ¹⁴B. Mühlschlegel, Z. Phys. 155, 313 (1959).
- ¹⁵J. Hasse and J. Lachmann, Z. Phys. 258, 136 (1973).
- ¹⁶W. H. Henkels and C. J. Kircher, IEEE Trans. Magn. MAG-13, 63 (1977).
- ¹⁷J. Halbritter, Z. Phys. 266, 209 (1974).
- ¹⁸M. A. Biondi and M. P. Garfunkel, Phys. Rev. 116, 853 (1959).
- ¹⁹M. A. Biondi and M. P. Garfunkel, Phys. Rev. 116, 862 (1959).
- ²⁰J. D. Leslie and D. M. Ginsberg, Phys. Rev. 133, 363 (1966).
- ²¹D. M. Ginsberg, Phys. Rev. 151, 241 (1966).
- ²²L. Leplae, Ph. D. thesis, University of Maryland, College Park (1962).
- ²³P. L. Richards and M. Tinkham, Phys. Rev. 119, 575 (1960).
- ²⁴D. M. Ginsberg and M. Tinkham, Phys. Rev. 118, 990 (1960).
- ²⁵S. L. Norman, Phys. Rev. 167, 393 (1968).
- ²⁶S. L. Norman, and D. H. Douglass, Phys. Rev. Lett. 18, 339 (1967).
- ²⁷W. Bauer, S. Giordano, and H. Hahn, J. Appl. Phys. 45, 5053 (1974).
- ²⁸A. Philipp and J. Halbritter, IEEE Trans. Magn. MAG-17, 951 (1981).
- ²⁹Y. Bruynseraede, D. Gorle, D. Leroy, and P. Morignot, Physica 54, 137 (1971).
- ³⁰P. Wilson, Interne Mitteilung SLAC-TN-70-35, Kernforschungs-Zenetrum Karlsruhe (1970).
- ³¹A. B. Pippard, in Advances in Electronics, edited by L. Marton (Academic, New York, 1954).

5957